



Computational fluid dynamics of a novel perfusion strategy during hybrid thoracic aortic repair

Giovanni Mariscalco MD, PhD^{1,2} | Gionata Fragomeni PhD, MD³ |
 Tryfon Vainas MD, PhD⁴ | Leonidas Hadjinikolaou FRCS¹ |
 Fausto Biancari MD, PhD⁵  | Umberto Benedetto MD, PhD⁶ | Antonio Salsano MD⁷ |
 Lina T. Gaudio PhD³ | Federica Jiritano MD⁸ | Pasquale Mastroberto MD⁸ |
 Giuseppe F. Serraino MD, PhD⁸ 

¹Department of Cardiac Surgery, Glenfield Hospital, University Hospitals of Leicester NHS Trust, Leicester, UK

²Department of Cardiovascular Sciences, University of Leicester, Leicester, UK

³Department of Surgical and Medical Sciences, Magna Graecia University of Catanzaro, Catanzaro, Italy

⁴Department of Vascular Surgery, Glenfield Hospital, University Hospitals of Leicester NHS Trust, Leicester, UK

⁵Department of Surgery, Heart Center, University of Turku, Turku, Finland

⁶School of Clinical Sciences, Bristol Heart Institute, University of Bristol, Bristol, UK

⁷Department of Integrated Surgical and Diagnostic Sciences (DISC), Division of Cardiac Surgery, University of Genoa, Genoa, Italy

⁸Department of Experimental and Clinical Medicine, Magna Graecia University of Catanzaro, Catanzaro, Italy

Correspondence

Giuseppe F. Serraino, MD, PhD, Department of Experimental and Clinical Medicine, Magna Graecia University of Catanzaro, 88100 Catanzaro, Italy.
 Email: serraino@unicz.it

Abstract

Background and Aim: To mitigate the risk of perioperative neurological complications during frozen elephant trunk procedures, we aimed to computationally evaluate the effects of direct cerebral perfusion strategy through a left carotid-subclavian bypass on hemodynamics in a patient-specific thoracic aorta model.

Methods: Between July 2016 and March 2019, 11 consecutive patients underwent frozen elephant trunk operation using the left carotid-subclavian bypass with a side graft anastomosis and right-axillary cannulation for systemic and brain perfusion. A multiscale model realized coupling three-dimensional computational fluid dynamics was developed and validated with in vivo data. Model comparison with direct antegrade cannulation of all epiaortic vessels was performed. Wall shear stress, wall shear stress spatial gradient, and localized normalized helicity were selected as hemodynamic indicators. Four cerebral perfusion flows were tested (6 to 15 mL/kg/min).

Results: Direct cerebral perfusion of the left subclavian bypass resulted in higher flow rates with augmented speeds in all epiaortic vessels in comparison with traditional perfusion model. At the level of the left vertebral artery (LVA), a speed of 22.5 vs 21 mL/min and mean velocity of 3.07 vs 2.93 cm/s were registered, respectively. With a cerebral perfusion flow of 15 mL/kg, lower LVA wall shear stress (1.596 vs 2.030 N/m²), and wall shear stress gradient (1445 vs 5882 N/m³) were observed. A less disturbed flow considering the localized normalized helicity was documented. No patients experienced neurological/spinal cord damages.

Conclusions: Direct perfusion of a left carotid bypass proved to be cerebroprotective, resulting in a more physiological and stable anterior and posterior cerebral perfusion.

KEYWORDS

aorta and great vessels, aortic repair, cardiovascular pathology, cerebral perfusion

1 | INTRODUCTION

Frozen elephant trunk (FET) represents a simplified treatment for complex diseases of the thoracic aorta that has rapidly gained popularity for its clinical and surgical advantages.^{1,2} FET allows for single-stage therapy in case of multilevel aortic diseases, favors the expansion of true lumen in type A acute dissections, and also offers a potential landing zone for subsequent transfemoral endovascular aortic repairs.^{1,3} However, in this context, the optimal cerebral protection strategy remains controversial, and FET procedure-related complications are not remote.¹⁻⁴ Neurological and spinal cord complications occur in 2.5% to 21% of treated patients.^{2,4}

To mitigate the risk of perioperative neurological complications during FET procedures, we have developed a modified cerebral perfusion strategy to both preserve the anterior and posterior cerebral circulation by simultaneous perfusion of the right axillary artery (RAA) and a left carotid-subclavian bypass. In the present study, through an image-based computational fluid dynamics (CFD) analysis, we aimed to assess the fluid dynamics and vascular biomechanical properties of this novel perfusion strategy to better understand the relationship between antegrade cerebral perfusion and the pathophysiology of neurological complications during aortic arch surgery.

2 | MATERIALS AND METHODS

2.1 | Study population

Between July 2016 and March 2018, 11 consecutive patients underwent "single-stage" operation with the Thoraflex hybrid stent-graft (Vascutek, Terumo, Inchinnan, UK) at University Hospital of Leicester, Glenfield Aortic Centre (UK) for the repair of complex thoracic aortic diseases involving the aortic arch and proximal descending thoracic aorta using our novel cerebral perfusion strategy. All patients data were prospectively collected in the National Institute for Cardiovascular Outcomes Research of the National Adult Cardiac Surgery Audit registry.⁵

2.2 | Operative technique

Total intravenous anesthesia was routinely administered. Both radial and left femoral arteries were cannulated to monitor the perfusion pressures to the brain and lower body part, especially during circulatory arrest and selective antegrade cerebral perfusion. In the same operating session and before sternotomy, a left carotid-subclavian bypass was constructed in all patients through a standard left supraclavicular incision, using an 8-mm Dacron graft (Vascutek, Terumo, Renfrewshire, Scotland). An additional 8-mm Dacron graft was then anastomosed ("T" configuration) to the same left carotid-subclavian bypass. This constituted the first arterial perfusion line for the institution of the cardiopulmonary bypass

(CPB). A second arterial cannulation site was also created through an 8-mm Dacron graft anastomosed to the RAA. After the median sternotomy, the innominate, the left common carotid (LCA), and the left subclavian arteries (LSA) were mobilized and encircled with tapes. After systemic heparinization, CPB was instituted through the two aforementioned perfusion lines. The venous drainage was achieved by cannulation of the right atrium. The left ventricle was vented through the right superior pulmonary vein. Myocardial protection was achieved using antegrade and retrograde administration of intermittent cold blood cardioplegia of Harefield Hospital formulation (IVEX Pharmaceuticals Ltd, Larne, Northern Ireland, UK). The ascending aortic aneurysm/dissection was then excised, and circulatory arrest was established at a target nasopharyngeal temperature of 23°C to 25°C. The innominate artery and LCA were then clamped and disconnected from the native aortic arch, while the LSA was permanently occluded at its origin. Therefore, cerebral perfusion was never interrupted, being maintained through the RAA and the left carotid-subclavian bypass perfusion lines. In all patients, near-infrared spectroscopy (INVOS cerebral oximeter; Somanetics Corporation, Troy, MI) was utilized to guide the cerebral perfusion, and target radial and femoral pressures were maintained at 50 to 70 and 20 to 30 mm Hg, respectively (perfusate flow: 8-10 mL/kg). The arch was then opened longitudinally, generally between the LCA and LSA origins. The Thoraflex hybrid graft was slightly reshaped to conform to the curvature of the descending thoracic aorta and deployed under direct vision, without using any guidewires. The hybrid device was selected according to the anatomic characteristics of the aortic arch/descending aorta and the type of lesion. Generally, 15 cm stent grafts were deployed in chronic atherosclerotic aneurysms, while 10 cm stent grafts were used in acute aortic syndromes. After the distal aortic arch reconstruction, the systemic perfusion through the side branch of the hybrid graft was recommenced. Subsequently, the proximal aortic repair was completed, and the cross-clamp removed. Reimplantation of the innominate artery and the LCA to the stent-graft branches was then performed on a beating heart, and the initial perfusion lines into the RAA and the left subclavian bypass were subsequently excluded. Cerebrospinal fluid drainage was never adopted.

2.3 | Computational modeling of the aorta

An image-based model of a 52-year-old male patient who undergone FET with the abovementioned cerebral perfusion configuration was created, using the postoperative computed tomography angiography of the entire thoracic aorta. The following two perfusion configurations were then compared, and the corresponding hemodynamic changes calculated, evaluating the blood flow in the aorta and supra-aortic vessels (Figure 1). Configuration 1 represented the traditional cerebral perfusion strategy using direct cannulation of the epi-aortic vessels including the LSA and was used for comparison.⁶⁻⁸ Configuration 2 (our novel perfusion configuration) consisted of the simultaneous cerebral and systemic perfusion through two 8-mm

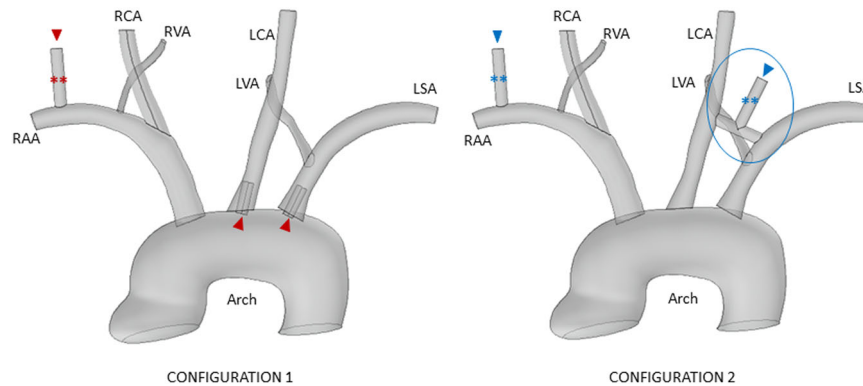


FIGURE 1 Patient-specific aortic model with geometrical reconstruction, including the supra-aortic vessels and the aortic arch. Both configuration models are represented. Arterial inflows are indicated by triangles. Asterisks identify the 8-mm Dacron grafts anastomosed to the RAA (configurations 1 and 2) and the left carotid-subclavian bypass (configuration 2). The left carotid-subclavian bypass is underlined by a blue circle. LCA, left carotid artery; LSA, left subclavian artery; LVA, left vertebral artery; RAA, right axillary artery; RCA, right carotid artery; RVA, right vertebral artery

Dacron grafts anastomosed to the RAA and the left carotid-subclavian bypass (Figure 1). Two interrelated mathematical models were adopted; one for the blood and the other for the vessel wall⁹⁻¹⁸ (see supporting information for Mathematical Model and Hemodynamic Indicators).

2.4 | CFD analysis

For the fluid-dynamic analysis, identical continuous flows were applied as for the inlet and outlet boundaries for each supra-aortic vessel, and for both configurations (Figure 2). The inlet boundary was set at the tip of the cannula, while the outlet was set in the output boundaries of supra-aortic vessels. At the inlet level, four different constant flows were tested for both configurations, mimicking different perfusion flow regimens. These values were derived from the European Association for Cardiothoracic Surgery survey on neuroprotection in aortic arch surgery.⁷ Perfusate flow was reported to be fairly consistent across 400 European centers in the average of 10 to 15 mL/kg/min.⁸ For a patient weighing 70 kg, we tested: (a) a total flow of 420 mL/min corresponding to 6 mL/kg/min (case A), (b) a total flow of 560 mL/min corresponding to 8 mL/kg/min (case B), a total flow of 700 mL/min corresponding to 10 mL/kg/min (case C) and, lastly, a total

flow of 1050 mL/min corresponding to 15 mL/kg/min (case D). For configuration 1, the total flow was divided by the three inlet cannulas, whereas for configuration 2 by two cannulas. The outputs were set equal to 60 mm Hg at the level of all supra-aortic vessels, corresponding to the usual cerebral perfusate pressure.⁹ Aortic walls and perfusion cannulas were assumed to be rigid, impermeable, and a no-slip condition ($v_{\text{wall}} = 0$) was adopted. For the numerical simulation, the postprocess and the visualization of numerical results, a finite-element-based commercial software package was used (COMSOL 4.3a, Inc, Stockholm, Sweden). A fine mesh consisting of tetrahedral elements was then generated. The blood flow was investigated in terms of velocity streamlines, pressure, and shear stress indices. A generalized minimal residual algorithm for solving a nonsymmetrical linear system of equations was used.¹⁹

3 | RESULTS

3.1 | Patient population

Eleven patients with a mean age of 63.9 ± 11.0 years (range, 47-79 years) underwent replacement of the aortic arch and repair of the descending aorta using the Thoraflex hybrid prosthesis, utilizing our

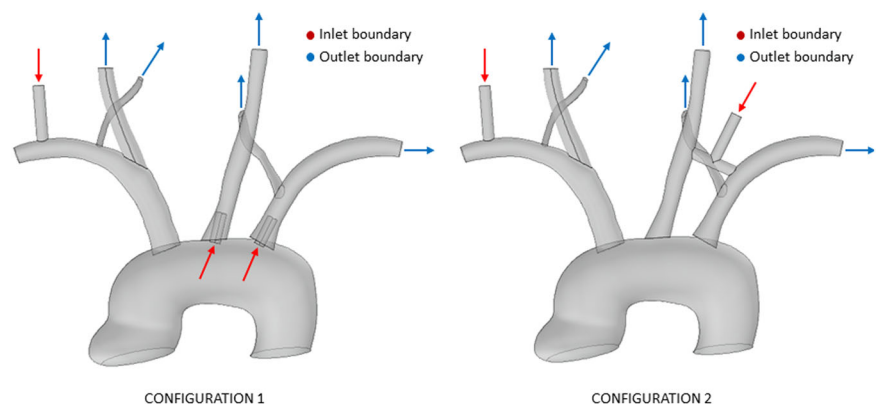


FIGURE 2 Geometrical reconstruction with related inlet and outlet boundaries for each supra-aortic vessel and for both configurations

TABLE 1 Baseline characteristics and outcomes of the patient population

Variable	Total (N = 11)
Demographic	
Age, y	63.9 (47-79)
Sex, male	7 (63.6)
Body mass index, kg/m ²	27.3 (22.5-35.7)
Cardiac status	
Emergent/urgent	6 (54.5)
NYHA IV/III	2 (18.2)
Prior myocardial infarction	1 (9)
Prior percutaneous coronary intervention	1 (9)
Coronary artery disease	3 (27.3)
Left ventricular ejection fraction	53.5 (40-70)
Pulmonary hypertension >35 mm Hg	2 (18.2)
Comorbidities	
Hypertension	9 (81.8)
COPD	1 (9)
Peripheral vascular disease	7 (63.6)
Creatinine	89.4 (50-122)
Aortic disease	
Aortic aneurysm	8 (72.7)
Type A acute aortic dissection	3 (27.3)
Operative details	
CPB time, min	219.8 (152-298)
Cross-clamp time, min	106.9 (80-177)
Lower body circulatory arrest	22.7 (21-35)
Concomitant surgical procedures	7 (63.6)
CABG	2 (18.2)
Valve surgery	5 (45.5)
Aortic root surgery	1 (9)
Thoraflex hybrid prosthesis size	
26/28 × 15 cm	2
28/20 × 15 cm	1
30/32 × 10 cm	1
30/36 × 15 cm	2
30/38 × 10 cm	1
30/38 × 15 cm	1
30/40 × 10 cm	1
32/40 × 15 cm	2
Outcomes and follow-up^a	
Hospital mortality	1 ^b (9)
CRRT	2 (18.2)
Re-exploration for bleeding	1 ^b (9)
Stroke	0
Spinal cord ischemia	0
Other complications	1 ^c
Mortality at F-U	0

Note: Data presented as median (minimum-maximum values) for continuous variables and n (%) for categorical variables. Abbreviations: CABG, coronary artery bypass grafting; COPD, chronic obstructive pulmonary disease; CPB, cardiopulmonary bypass; CRRT, continuous renal replacement therapy; F-U, follow-up; NYHA, New York Heart Association (class).

^aMedian follow-up: 18 mo (2-30).

^bRelated to uncontrolled bleeding after pacemaker implantation at 1 wk from the operation.

^cProximal anastomosis pseudoaneurysm at 6 mo from the operation.

technique as the only cerebral perfusion strategy. Baseline operative and postoperative characteristics of the patient population are summarized in Table 1. The follow-up interval ranged from 2 to 30 months with a median of 18 months. In brief, the treated aortic lesions included chronic atherosclerotic or dissecting aneurysms (n = 8) and acute aortic syndromes (n = 3). None of the enrolled patients had previous cardiac, thoracic, or abdominal aortic surgery. There was no history of any cerebrovascular accidents documented. The cumulative CPB time was 219.4 ± 39.8 minutes, and lower body circulatory arrest time was 22.7 ± 13.5 minutes. Concomitant cardiac procedures were performed in seven (64%) cases. One patient died after 15 days for uncontrolled bleeding after pacemaker implantation for perioperative complete atrioventricular block. None of the enrolled patients experienced any temporary/permanent neurological or spinal cord injuries. At long term follow-up, all patients were alive (Table 1).

3.2 | Computational modeling results

Figure 3A,B shows the trend of the velocities with a maximum perfusion flow of 1050 mL/min (15 mL/kg). Configuration 1 resulted in lower flow rates with reduced speeds in the vertebral arteries, LCA and LSA compared to configuration 2. The calculated flow in the left vertebral artery (LVA) for configuration 1 was 21 mL/min with a mean velocity of 2.93 cm/s, while configuration 2 demonstrated higher values equal to 22.5 mL/min with a mean velocity of 3.07 cm/s. In configuration 1, the presence of vortices at the level of vertebral arteries was also more frequently observed than in configuration 2 (Figure 3C,D). The percentage of variations in term of reduction of flow and mean velocity in the vertebral arteries were also calculated. The values of the three different perfusate flows (cases A, B, and C) were compared with those of a perfusate flow of 1050 mL/min (case D). Table 2 reports the variations in terms of reduction of flow and mean velocity in the vertebral arteries for both configuration models. Again, configuration 1 resulted in less stability during cannula flow variations, causing a higher percentage of variation at the vertebral arteries level.

Figure 4 shows the results of the wall shear stress (WSS) calculation in both configuration models. Configuration 1 demonstrated higher values at cannula level as a consequence of greater flow. With a perfusate flow of 1050 mL/min, a WSS of 2.030 N/m² was observed at the level of LVA in the configuration 1, while a lower WSS (1.596 N/m²) was encountered in the configuration 2. Higher WSS values are associated with an increased risk of endothelial damage and disruption. Similarly, in configuration 1, the wall shear stress gradient (WSSG), calculated as the maximum value along the vertebral artery surface, was 5882 N/m³. In configuration 2, the WSSG value was lower and equal to 1445 N/m³. Results obtained for cases A, B, and C were finally compared with those of case D, and percentages of variations were then calculated (Table 3). Configuration 1 brought a considerable WSS reduction (up to 80%) with respect to the maximum flow value. Finally, considering the

FIGURE 3 Velocity streamlines (m/s) recorded in all supra-aortic vessels for the cerebral perfusion model obtained with configuration 1 (A and C) and with configuration 2 (B and D). C and D, Details of velocity streamlines at the level of left vertebral arteries. Colors denote velocity values, from smallest (blue) to highest (red)

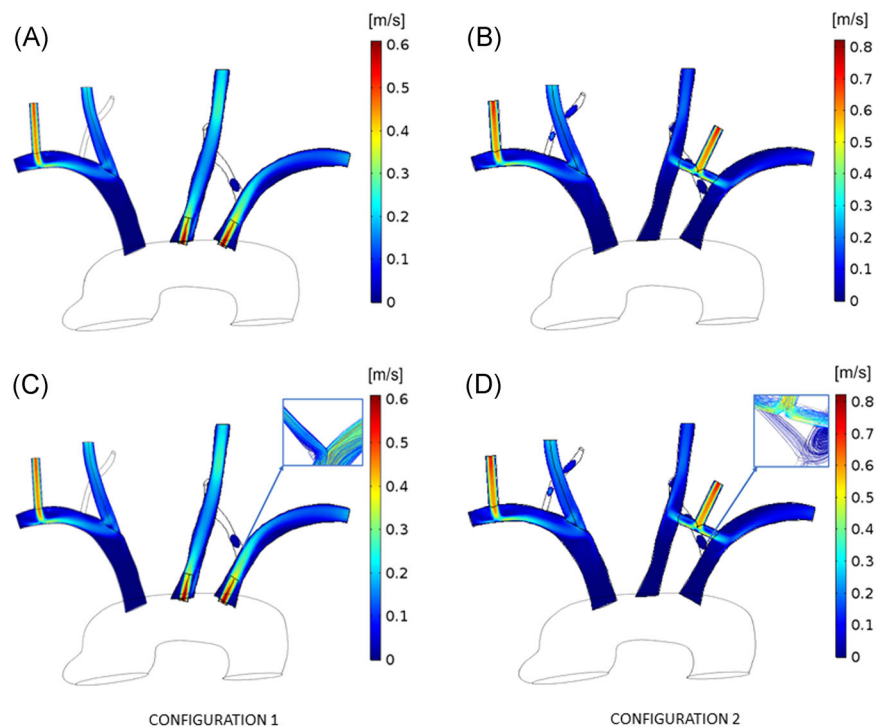


TABLE 2 Percentage variations of flow and velocity in configurations 1 and 2

Perfusate flow, mL/min	Configuration 1		Configuration 2	
	Flow mL/min, %	Velocity mean cm/s, %	Flow mL/min, %	Velocity mean cm/s, %
Case A (420 mL/min) vs case D	6.9, 67%	1.0, 67%	7.9, 65%	1.2, 65%
Case B (560 mL/min) vs case D	10.9, 48%	1.5, 48%	13.5, 40%	1.9, 40%
Case C (700 mL/min) vs case D	14.1, 33%	2.0, 33%	16.2, 28%	2.2, 28%

Note: Different perfusate flows are compared with a maximum perfusate flow of 1050 mL/min (case D).

localized normalized helicity at the vertebral level, configuration 1 resulted in a more disturbed flow than configuration 2 (Figure 5).

4 | CONCLUSION

Several methods for cerebral perfusion have been adopted to address aortic arch and descending aortic disease repairs, including

metabolic suppression with anesthetic agents, antegrade and retrograde cerebral perfusion (ACP), and hypothermic circulatory arrest.^{6-8,20} In a recent survey, reporting the current trends in cannulation and neuroprotection during aortic arch surgery in Europe, bilateral, and unilateral ACPs were the most commonly utilized methods, accounting for 53% and 38% of strategies in the acute setting, and for 65% and 33% in chronic aortic conditions, respectively.⁸ Although these operative strategies are directed at

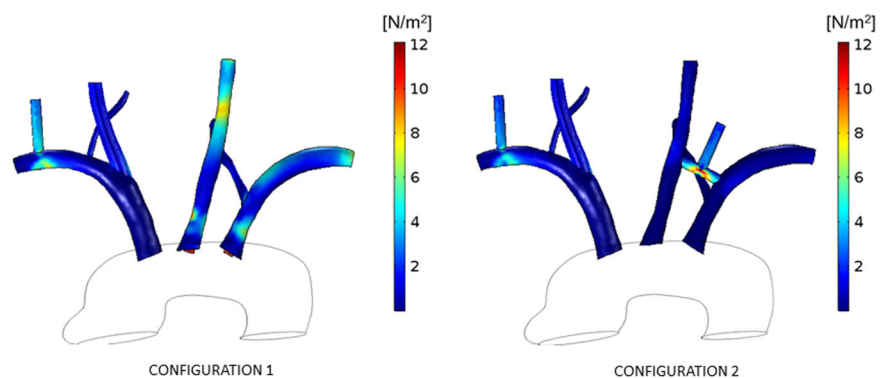


FIGURE 4 Wall shear stress (WSS) distribution recorded in all supra-aortic vessels during cerebral perfusion for configurations 1 and 2. Colors denote WSS values, from smallest (blue) to highest (red)

TABLE 3 Percentage variations of WSS and WSSG in configurations 1 and 2

Perfusate flow, mL/min	Configuration 1		Configuration 2	
	WSS N/m ² , %	GWSS N/m ³ , %	WSS N/m ² , %	GWSS N/m ³ , %
Case A (420 mL/min) vs case D	0.4, 80%	411, 93%	0.7, 61%	463, 68%
Case B (560 mL/min) vs case D	0.7, 64%	1235, 79%	0.9, 47%	607, 58%
Case C (700 mL/min) vs case D	1.0, 51%	3529, 60%	1.1, 33%	766, 47%

Note: Different perfusate flows are compared with a maximum perfusate flow of 1050 mL/min (case D).

Abbreviations: GWSS, gradients of wall shear stresses; WSS, wall shear stress; WSSG, wall shear stress gradient.

reducing operative mortality and morbidity, the occurrence of temporary and permanent neurologic deficits remains high.¹⁻⁴ Even in elective proximal arch surgeries, a 6% rate of paraplegia is encountered, highlighting the need for further measures to reduce this devastating complication, especially in the case of more time demanding extensive aortic repairs.²¹ In this context, additional perfusion of LSA seems to be beneficial, particularly in critical vascular conditions, such as concomitant carotid dissections, acute right vertebral artery occlusion, dominant LVA, or inadequate intracranial arterial communications.²²⁻²⁷ Notably, studies reporting on outcomes after thoracic endovascular aortic repair with overstenting of the LSA have demonstrated an increased risk of left-hemispheric stroke and permanent paraplegia.²⁸⁻³⁰ Furthermore, the perfusion of the LVA through the LSA is of utmost importance in the presence of posterior anomalies of the Willis circle (type IA and type IIA variations).²⁷

Moriyama et al^{23,24} first introduced the selective perfusion of the LSA during the repair of the descending thoracic and thoracoabdominal aortic aneurysms under deep hypothermia. Avoiding retrograde perfusion, they did not encounter any brain injury.²⁴ Kurisu et al²⁵ described the use of bilateral cerebral perfusion through cannulation of both axillary arteries in 12 patients undergoing aortic arch surgery. Although this was a preliminary and limited series, the authors did not observe any temporary and permanent neurologic deficits, nor paraplegia.²⁵ Similarly, Xydias et al²⁶ did not report any neurological or paraplegia complication during aortic arch reconstructions with the routine use of a carotid-subclavian arterial bypass.

To minimize cerebral ischemia and the risk of inadequate cerebral perfusion, preserving both anterior and posterior cerebral circulation, we recently introduced the use of a perioperative left carotid-subclavian bypass as CPB arterial inflow, warranting the simultaneous perfusion of the LCA, LSA, and LVA. In the present study, we were able to demonstrate through an image-based CFD analysis that our modified cerebral perfusion configuration resulted in a more physiological and stable cerebral blood perfusion. Our excellent neurological outcomes also corroborate the image-based CFD data, although we are conscious that this is a preliminary and limited patient series.

Our cerebral configuration presents several advantages. First, the simultaneous perfusion of the LCA, LSA, and LVA maintain the complete blood circulation in the anterior and posterior cerebral circle, avoiding the risk of inadequate perfusion in the presence of undetected Willis anomalies. This technique is of importance in the acute setting when an accurate and immediate intracranial arterial imaging is not feasible as in the case of an impending aortic rupture. Second, a direct LSA anastomosis through median sternotomy is often challenging, requiring unduly prolonged cerebral ischemia time and poor LSA visualization with the risk of uncontrolled bleeding, especially in case of a dissected and fragile LSA.³¹ Third, the distal FET anastomosis can be easily performed in zone 0 and 1 with excellent visualization, reducing the cerebral ischemia time and favoring a better and direct hemostatic control. Fourth, the avoidance of direct cannulation of the supra-aortic vessels greatly reduces the risks of cerebrovascular accidents resulting from air embolism or dislodgement of atherosclerotic debris.^{31,32} In acute aortic dissection involving the aortic arch vessels, direct carotid cannulation

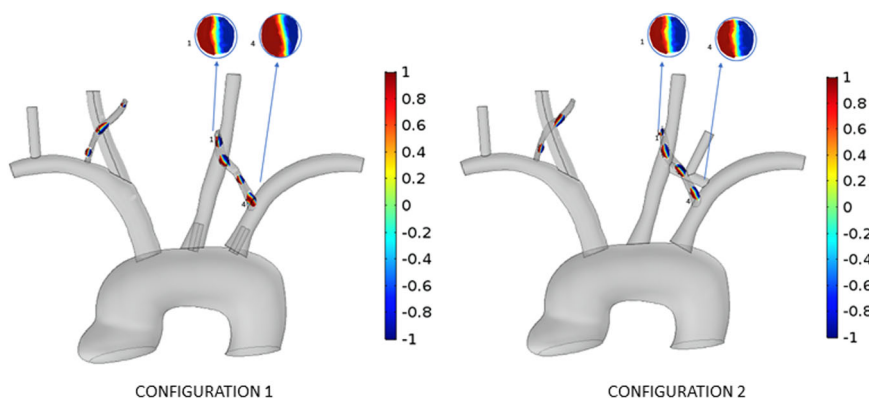


FIGURE 5 Localized normalized helicity (LNH) distribution recorded in all supra-aortic vessels during cerebral perfusion for configurations 1 and 2. Colors denote LNH values, from negative (blue) to positive (red)

could potentially lead to the damage of the arterial wall intima, causing bleeding complications or serious malperfusion.³¹ The latter can also be caused by improper insertion of the perfusion carotid cannulas.³³ Finally, our technique is fully compatible with other aortic arch and descending repairs and aortic root reconstructions.

The configuration of our cerebral perfusion strategy is patho-physiologically justified by clinical and experimental evidence, suggesting that spinal cord perfusion does not principally depend on a single branch artery of the descending thoracic aorta, the so-called artery of Adamkiewicz.^{34,35} It has been demonstrated that spinal cord perfusion is supported by an extensive integrated collateral arterial network, including the segmental and epidural arteries, and the anterior spinal artery. All these vessels are interconnected with the subclavian arteries cranially, and the hypogastric arteries caudally.³⁵ The result is an extensive collateral compensatory flow to spinal cord even when some collaterals are irreparably compromised or in case of an anatomically incomplete circle of Willis.^{22,35} In rats, the bilateral direct ACP alone resulted in perfusion of only 30% of the spinal cord through to the retrograde flow of the vertebrobasilar system. Perfusion of the subclavian arteries alone resulted in greater spinal cord perfusion (up to 40%).²² The simultaneous bilateral ACP with at least one of the subclavian arteries was demonstrated to provide much better perfusion to both the spinal cord and the brain.²³ This evidence is consonant with our image-based CFD analysis that demonstrated a more physiological and stable cerebral blood perfusion when the carotid-subclavian bypass is used as direct arterial inflow for cerebral perfusion.

Certainly, the present study is limited by its nonrandomized and observational nature, in addition to the limited patient population. We used idealized boundary conditions for investigating the impact of our cerebral perfusion configuration. Possible bias originating by the cardiac function of the patients as well as concomitant cardiac diseases, and hypertension were not considered in our calculations. Finally, we did not use magnetic resonance imaging or computerized tomography scans to document any encephalopathy or clinically silent cerebral diseases.

In conclusion, the additional direct perfusion of a left carotid-subclavian bypass provides a more physiological and stable cerebral perfusion, warranting an adequate and complete anterior and posterior cerebral circulation. This technique may decrease the risk of neurological and spinal cord complications associated with aortic arch and descending aortic repairs, especially in case of undetected vascular compromises such as a dominant LVA, carotid artery disease, or inadequate intracranial arterial communication.

ACKNOWLEDGMENTS

The author would like to thank Zein El Dean for his assistance in important language and grammar-editing services.

CONFLICT OF INTERESTS

The authors declare that there are no conflict of interests.

AUTHOR CONTRIBUTIONS

GM, GF, LTG, PM, and GFS contributed in concept/design, data analysis/interpretation, drafting article, critical revision of article, approval of article, statistics, and data collection. TV, LH, FB, UB, AS, and FJ contributed in concept/design, data interpretation, drafting article, critical revision of article, and approval of the article.

ORCID

Fausto Biancari  <http://orcid.org/0000-0001-5028-8186>

Giuseppe F. Serraino  <http://orcid.org/0000-0002-4804-9570>

REFERENCES

- Shrestha M, Bachet J, Bavaria J, et al. Current status and recommendations for use of the frozen elephant trunk technique: a position paper by the vascular domain of EACTS. *Eur J Cardiothorac Surg.* 2015;47:759-769.
- Tian DH, Wan B, Di Eusano M, Black D, Yan TD. A systematic review and meta-analysis on the safety and efficacy of the frozen elephant trunk technique in aortic arch surgery. *Ann Cardiothorac Surg.* 2013;2:581-591.
- Shrestha M, Martens A, Kaufeld T, et al. Single-centre experience with the frozen elephant trunk technique in 251 patients over 15 years. *Eur J Cardiothorac Surg.* 2017;52:858-866.
- Hanif H, Dubois L, Ouzounian M, et al. Aortic arch reconstructive surgery with conventional techniques vs frozen elephant trunk: a systematic review and meta-analysis. *Can J Cardiol.* 2018;34:262-273.
- <http://www.ucl.ac.uk/nicor/audits/adultcardiac/documents/datasets/NACSAdatasetV4.1.2>. Accessed April 30, 2015.
- Di Eusano M, Schepens MA, Morshuis WJ, Di Bartolomeo R, Pierangeli A, Dossche KM. Antegrade selective cerebral perfusion during surgery of the thoracic aorta: factors influencing survival and neurologic outcome in 413 patients. *J Thoracic Cardiovasc Surg.* 2002;124:1080-1086.
- Dossche KM, Schepens MA, Morshuis WJ, Waanders FG. Bilateral antegrade selective cerebral perfusion during surgery on the proximal thoracic aorta. *Eur J Cardiothorac Surg.* 2000;17:462-467.
- De Paulis R, Czerny M, Weltert L, et al. Current trends in cannulation and neuroprotection during surgery of the aortic arch in Europe. *Eur J Cardiothorac Surg.* 2015;47:917-923.
- Quarteroni A, Formaggia L. Modelling of living systems. In: Ciarlet PG, Lions JL, eds. *Mathematical Modelling and Numerical Simulation of the Cardiovascular System. Handbook of Numerical Analysis Series.* Amsterdam, The Netherlands: Elsevier; 2004:3-127.
- McDonald DA. Contours of pressure and flow waves in arteries. In: Nichols WW, O'Rourke MF, eds. *Blood Flow in Arteries.* 3rd ed. London, UK: Edward Arnold Ltd; 1990.
- Fung YC. The flow properties of blood. In: Fung YC, ed. *Biomechanics: Mechanical Properties of Living Tissues.* New York, NY: Springer-Verlag; 1993:321-384.
- Gramigna V, Caruso MV, Rossi M, Serraino GF, Renzulli A, Fragomeni G. A numerical analysis of the aortic blood flow pattern during pulsed cardiopulmonary bypass. *Comput Methods Biomech Biomed Engin.* 2015;18:1574-1581.
- Caruso MV, Gramigna V, Renzulli A, Fragomeni G. Computational analysis of aortic hemodynamics during total and partial extra-corporeal membrane oxygenation and intra-aortic balloon pump support. *Acta Bioeng Biomech.* 2016;18:3-9.

14. Zhang JM, Chua LP, Ghista DN, Yu SC, Tan YS. Numerical investigation and identification of susceptible sites of atherosclerotic lesion formation in a complete coronary artery bypass model. *Med Biol Eng Comput.* 2008;46:689-699.
15. Peiffer V, Sherwin SJ, Weinberg PD. Does low and oscillatory wall shear stress correlate spatially with early atherosclerosis? A systematic review. *Cardiovasc Res.* 2013;99:242-250.
16. Dolan JM, Kolega J, Meng H. High wall shear stress and spatial gradients in vascular pathology: a review. *Ann Biomed Eng.* 2013;41:1411-1427.
17. Huo Y, Wischgoll T, Kassab GS. Flow patterns in three-dimensional porcine epicardial coronary arterial tree. *Am J Physiol Heart Circ Physiol.* 2007;293:H2959-H2970.
18. Garcia J, Barker AJ, Collins JD, Carr JC, Markl M. Volumetric quantification of absolute local normalized helicity in patients with bicuspid aortic valve and aortic dilatation. *Magn Reson Med.* 2017;78:689-701.
19. Saad Y, Schultz MH. GMRES: a generalized minimal residual algorithm for solving nonsymmetric linear systems. *SIAM J Sci Stat Comput.* 1986;7:856-69.
20. Apostolakis E, Akinosoglou K. The methodologies of hypothermic circulatory arrest and of antegrade and retrograde cerebral perfusion for aortic arch surgery. *Ann Thorac Cardiovasc Surg.* 2008;14:138-148.
21. Luehr M, Peterss S, Zierer A, et al. Aortic events and reoperations after elective arch surgery: incidence, surgical strategies and outcomes. *Eur J Cardiothorac Surg.* 2018;53:519-524.
22. Al-Ali S, Chen BS, Papali'i-Curtin AT, et al. Adequacy of brain and spinal blood supply with antegrade cerebral perfusion in a rat model. *J Thorac Cardiovasc Surg.* 2011;141:1070-1076.
23. Moriyama Y, Taira A, Hisatomi K, Iguro Y. Left subclavian artery as a site of proximal aortic perfusion for hypothermic repair of thoracic and thoracoabdominal aneurysms. *J Thorac Cardiovasc Surg.* 1999;117:408-409.
24. Moriyama Y, Iguro Y, Hisatomi K, Yotsumoto G, Yamamoto H, Toda R. Thoracic and thoracoabdominal aneurysm repair under deep hypothermia using subclavian arterial perfusion. *Ann Thorac Surg.* 2001;71:29-32.
25. Kurisu K, Ochiai Y, Hisahara M, Tanaka K, Onzuka T, Tominaga R. Bilateral axillary arterial perfusion in surgery on thoracic aorta. *Asian Cardiovasc Thorac Ann.* 2006;14:145-149.
26. Xydas S, Wei B, Takayama H, et al. Use of carotid-subclavian arterial bypass and thoracic endovascular aortic repair to minimize cerebral ischemia in total aortic arch reconstruction. *J Thorac Cardiovasc Surg.* 2010;139:717-722.
27. Papantchev V, Stoinova V, Aleksandrov A, et al. The role of Willis circle variations during unilateral selective cerebral perfusion: a study of 500 circles. *Eur J Cardiothorac Surg.* 2013;44:743-753.
28. Luehr M, Etz CD, Berezowski M, et al. Outcomes after thoracic endovascular aortic repair with overstenting of the left subclavian artery. *Ann Thorac Surg.* 2018;S0003-4975(18):31711-31719.
29. Bradshaw RJ, Ahanchi SS, Powell O, et al. Left subclavian artery revascularization in zone 2 thoracic endovascular aortic repair is associated with lower stroke risk across all aortic diseases. *J Vasc Surg.* 2017;65:1270-1279.
30. Mariscalco G, Piffaretti G, Tozzi M, et al. Predictive factors for cerebrovascular accidents after thoracic endovascular aortic repair. *Ann Thorac Surg.* 2009;88:1877-1881.
31. Ueda T, Shimizu H, Ito T, et al. Cerebral complications associated with selective perfusion of the arch vessels. *Ann Thorac Surg.* 2000;70:1472-1477.
32. Di Eusano M, Wesselink RMJ, Morshuis WJ, Dossche KM, Schepens MA. Deep hypothermic circulatory arrest and antegrade selective cerebral perfusion during ascending aorta-hemiarch replacement: a retrospective comparative study. *J Thorac Cardiovasc Surg.* 2003;125:849-854.
33. Orihashi K, Sueda T, Okada K, Imai K. Malposition of selective cerebral catheter is not a rare event. *Eur J Cardiothorac Surg.* 2005;27:644-648.
34. Adamkiewicz A. Die Blutgefasse des Menschlichen Ruckenmarkes. Krakau. 1881.
35. Griep EB, Di Luozzo G, Schray D, Stefanovic A, Geisbüs S, Griep RB. The anatomy of the spinal cord collateral circulation. *Ann Cardiothorac Surg.* 2012;1:350-357.

SUPPORTING INFORMATION

Additional supporting information may be found online in the Supporting Information section.

How to cite this article: Mariscalco G, Fragomeni G, Vainas T, et al. Computational fluid dynamics of a novel perfusion strategy during hybrid thoracic aortic repair. *J Card Surg.* 2020;1-8. <https://doi.org/10.1111/jocs.14436>